Geophysical Research Letters

RESEARCH LETTER
10.1029/2018GL078990

South Atlantic Forced Multidecadal Teleconnection to the Midlatitude South Indian Ocean

Jiaqing Xue[1,2,3], Cheng Sun[4], Jianping Li[2,4], and Jiangyu Mao[1]

[1]State Key Laboratory of Numerical Modeling for Atmospheric Sciences and Geophysical Fluid Dynamics, Institute of Atmospheric Physics, Chinese Academy of Sciences, Beijing, China, [2]Laboratory for Regional Oceanography and Numerical Modeling, Qingdao National Laboratory for Marine Science and Technology, Qingdao, China, [3]College of Earth Science, University of Chinese Academy of Sciences, Beijing, China, [4]College of Global Change and Earth System Science, Beijing Normal University, Beijing, China

Key Points:
- A multidecadal transbasin SST teleconnection is identified between the South Atlantic and the midlatitude south Indian Ocean (MSIO)
- Decadal fluctuation in MSIO SST is remotely synchronized by South Atlantic multidecadal variability
- This transbasin teleconnection is initiated by an atmospheric bridge from the South Atlantic and is amplified by a local air-sea feedback

Supporting Information:
- Supporting Information S1

Correspondence to:
J. Li,
ljp@bnu.edu.cn

Citation:
Xue, J., Sun, C., Li, J., & Mao, J. (2018). South Atlantic forced multidecadal teleconnection to the midlatitude south Indian Ocean. *Geophysical Research Letters*, *45*, 8480–8489. https://doi.org/10.1029/2018GL078990

Received 20 JAN 2018
Accepted 9 JUL 2018
Accepted article online 16 JUL 2018
Published online 18 AUG 2018

Abstract Sea surface temperature (SST) in the midlatitude south Indian Ocean (MSIO) exhibits prominent multidecadal fluctuations that have profound climate impacts for regions around the Indian Ocean. Observational analysis suggests that these multidecadal fluctuations can be explained by remote forcing from South Atlantic multidecadal variability. A suite of Atlantic Pacemaker experiments performs well in reproducing the observed MSIO SST multidecadal variation and its association with the South Atlantic. This transbasin covariability can be described by an atmospheric bridge mechanism, in which South Atlantic multidecadal variability-related SST warming weakens regional meridional circulation over the South Atlantic, suppressing convection over tropical Africa. The reduced diabatic heating then drives a cold atmospheric Kelvin wave that penetrates into the tropical Indian Ocean, leading to an anomalous cyclonic circulation there that weakens the westerlies over the MSIO and subsequently triggers the warming of MSIO. This initial warming is further amplified by local SST-water vapor positive feedback over the MSIO.

Plain Language Summary The midlatitude south Indian Ocean (MSIO) plays a critical role in global energy distribution and is one of the major windows through which the heat penetrates into deep ocean layers during the global warming hiatus periods. The MSIO sea surface temperature (SST) exhibits pronounced decadal variations, which have widespread climate impacts, affecting the East Asian summer monsoon and Indian monsoon rainfall. However, the underlying mechanism governing this decadal variability remains unclear. In this paper, we find that decadal fluctuation in MSIO SST is remotely synchronized by South Atlantic multidecadal variability (SAMV) based on both observational products and Atlantic Pacemaker experiments. This transbasin covariability is triggered by an atmospheric bridge emanating from the South Atlantic and further amplified by local positive air-sea feedback over the MSIO. This new insight into SAMV-MSIO SST connection not only extends our knowledge of the climatic impacts of SAMV but also has implications for interpreting the decadal variability in the East Asian summer monsoon.

1. Introduction

About one third of the world's population lives in countries surrounding the Indian Ocean, most of which are developing countries that are particularly vulnerable to climate variability and change. Thus, a better understanding of Indian Ocean variability has the potential to benefit the livelihood of those in regions bordering the ocean. Overlying the secular warming trend, pronounced decadal variations are present in Indian Ocean sea surface temperature (SST) (Cole et al., 2000; Han et al., 2014; Krishnamurthy & Krishnamurthy, 2016). Over the tropics, Indian Ocean decadal variability is dominated by a basin-wide warming/cooling pattern that is associated with remote forcing by the Interdecadal Pacific Oscillation (Dong et al., 2016; Han et al., 2014; Tozuka et al., 2007). Moreover, there are strong evidences indicating the existence of a noticeable SST decadal fluctuation in the midlatitude south Indian Ocean (MSIO; south of 30°S; Allan et al., 1995; Reason, 2000). The decadal variation in MSIO SST has widespread climate impacts, affecting the East Asian summer monsoon (Xue, 2001; Zhang et al., 2017), Indian monsoon rainfall (Feudale & Kucharski, 2013), and tropical cyclone activity (Cheung et al., 2015). Furthermore, the MSIO also plays a critical role in global energy distribution, as more heat is observed to penetrate into deep ocean layers of the MSIO during the global warming hiatus periods (Lee et al., 2015; Trenberth & Fasullo, 2013). However, decadal fluctuation in MSIO SST cannot be explained by the Interdecadal Pacific Oscillation signal (supporting information Figure S1), and the exact mechanism governing this variability remains to be thoroughly explored.

The South Atlantic Ocean, characterized by distinct ocean dynamic processes, plays an important role in energy distribution as a component of the global conveyor (Marshall & Speer, 2012). Recently, much work has focused on decadal fluctuations in South Atlantic SST and their climate impacts (Le Bars et al., 2016; Lopez, Dong, Lee, & Campos, 2016; Morioka et al., 2015; Nnamchi et al., 2016; Xue et al., 2018). Several physical mechanisms have been proposed to explain the South Atlantic decadal variability. Particularly, it was reported that decadal variations in South Atlantic Meridional Overturning Circulation can produce lagged SST signals over the South Atlantic through heat convergence/divergence, which has predictive implications for decadal variability in South Atlantic SST (Lopez, Dong, Lee, & Goni, 2016). Moreover, the midlatitude South Atlantic is a region of active mesoscale eddies, and the nonlinear eddy-mean flow interactions can generate intrinsic decadal variability in South Atlantic temperature (Le Bars et al., 2016). In addition to ocean processes, local air-sea interactions over the South Atlantic can also induce the SST decadal variability (Venegas et al., 1998; Wainer & Venegas, 2002). For example, Venegas et al. (1998) suggested that the decadal variability in South Atlantic SST is associated with the horizontal heat advection by ocean circulations and surface heat flux exchanges through air-sea interactions.

A previous study by Venegas et al. (1998) noted that decadal SST variation in the Indian Ocean covaries with that in the South Atlantic; however, the underlying mechanism for this decadal-scale teleconnection is not revealed. Since the Southern Ocean is an open basin, on the one hand, the ocean circulation can play important roles in linking the variability in the South Atlantic to that in the Indian Ocean (Le Bars et al., 2016; Morioka et al., 2015, 2017). Recently, Morioka et al. (2017) found that the decadal temperature variability in the South Atlantic can slowly propagate eastward into the Indian Ocean through oceanic Rossby waves along the Antarctic Circumpolar Current. Nevertheless, the possible role of the atmosphere in linking the decadal variability in these two oceanic regions remains unknown. In this study, we explore the transbasin teleconnection in SST decadal variability between the South Atlantic and the MSIO. Based on a suite of Atlantic Pacemaker experiments, an atmospheric bridge mechanism is proposed to explain this decadal-scale teleconnection.

2. Data and Methodology

2.1. Data Sets

SST data employed in the present study are taken from the Hadley Centre SST (HadISST) data set with 1° latitude by 1° longitude resolution covering the period 1900–2013 (Rayner et al., 2003). Because of large uncertainties in atmospheric data over the middle to high latitudes of the Southern Hemisphere before 1948, atmospheric data from the National Centers for Environmental Prediction and Atmospheric Research reanalysis 1 (Kalnay et al., 1996) and the Twentieth Century Reanalysis Version 2 (Compo et al., 2011) data sets, which include sea level pressure (SLP) and surface wind fields, are analyzed only for the post-1948 period. Anomalies for all variables are computed as deviations from the 1961–1990 climatology and are converted to annual-mean values for analysis. A least squares method is used to remove long-term linear trends, and an 11-year running mean is applied to extract decadal signals.

2.2. Statistical Method

We use a two-tailed Student's *t* test to determine the significance levels of linear correlation and regression. To consider the influence of autocorrelations on degrees of freedom, the effective number of degrees of freedom N^{eff} is thus calculated based on the following approximation:

$$\frac{1}{N^{\text{eff}}} \approx \frac{1}{N} + \frac{2}{N}\sum_{j=1}^{N}\frac{N-j}{N}\rho_{XX}(j)\rho_{YY}(j) \tag{1}$$

in which N is the sample size, and $\rho_{XX}(j)$ and $\rho_{YY}(j)$ separately represent the autocorrelations of time series X and Yat time lag j. (Li et al., 2013; Sun et al., 2016).

2.3. Numerical Experiments

The numerical model employed here is the International Centre for Theoretical Physics atmospheric general circulation model (ICTPAGCM) coupled to a thermodynamic slab ocean model (SOM). The intermediate ICTPAGCM adopts T30 horizontal spectral truncation and includes eight vertical levels. For the SOM, a heat

flux correction is applied to climatological SST. The mixed-layer depth d_o varies between 40 m (d_{omin}) in the tropical and 60 m (d_{omax}) in extratropical regions following $d_o = d_{omax} + (d_{omin} - d_{omax})\cos(\text{lat})^3$. Mixed-layer temperature variation is determined by net surface heat fluxes into the ocean (i.e., the sum of shortwave and longwave radiation and sensible and latent heat fluxes; Kucharski, Ikram, et al., 2016; Kucharski, Parvin, et al., 2016; Sun et al., 2017).

The Atlantic in this study is defined as the domain of 60°S–60°N, 70°W–20°E, while basins outside the Atlantic are called the Indo-Pacific region. Two sets of experiments are performed to investigate Atlantic forcing on atmospheric and SST variations over the Indo-Pacific region. The ATL_VARMIX experiment is run with the ICTPAGCM coupled to the mixed-layer SOM over the Indo-Pacific region and with observational SST from the HadISST prescribed over the Atlantic basin (i.e., Atlantic Pacemaker experiment). To prevent instability, a buffer zone of 7.5° is set between the slab ocean and prescribed-SST regions. Results of the ATL_VARMIX simulation reflect the combined effects of Atlantic SST forcing and air-sea coupling over the Indo-Pacific region. A similar experiment, ATL_VARAGCM, is performed with the ICTPAGCM forced by observational SST over the Atlantic and by climatological SST over the Indo-Pacific region. In contrast to the ATL_VARMIX, the ATL_VARAGCM experiment is used to isolate the direct atmospheric impacts of Atlantic forcing excluding the feedback from the ocean (Sun et al., 2017). Both simulations are integrated from 1872 to 2013 and contain five ensemble members created by restarting the model with small initial perturbations. The years 1872–1899 of all integrations are used as spin-up, and only results from the remaining period 1900–2013 are analyzed. All analyses are based on the average of five ensemble members.

3. Results

The southwestern portion of the South Atlantic Ocean exhibits the strongest decadal variability in the basin. The average SST anomalies over the southwest South Atlantic (25°–50°S, 50°–10°W) can thus be employed to define the South Atlantic multidecadal variability (SAMV) index (Xue et al., 2018), which performs well in characterizing decadal variability in South Atlantic SST (supporting information Figure S2). Figure 1a presents the decadal-scale correlation pattern between the SAMV index and SST field over the Atlantic and Indian Ocean regions, based on the HadISST data set. This pattern highlights a large area of significant positive correlations in the MSIO, particularly for the key region indicated by the green box. So, the MSIO SST index can be constructed from average SST anomalies over the key domain of 30°–45°S, 50°–80°E in the MSIO. Figure 1b gives normalized time series of detrended SAMV and MSIO SST indices during the period 1900–2013. The fluctuation in MSIO SST is found to be strongly in phase with that in SAMV ($r = 0.54$ for the unfiltered time series and $r = 0.84$ for the 11-year running mean time series, both above the 95% confidence level). The power spectra of detrended SAMV and MSIO SST indices both show significant quasi-40-year peaks, indicating that SST fluctuations in these two oceanic regions occur predominantly on multidecadal time scales. Meanwhile, the cross-spectrum analysis shows that SST variations in these two regions are coherent at quasi-40-year periods with the South Atlantic leading by about 2 years (supporting information Figure S3), which indicates that the South Atlantic may play a forcing role in the decadal transbasin SST teleconnection. The decadal-scale positive correlation between the SAMV and MSIO SST indices is further demonstrated to be robust and unaffected by the size of the smoothing window (supporting information Figure S4). To better reveal the spatial patterns of SAMV-MSIO SST decadal teleconnection, Figure 1c also shows the correlation map between the 11-year running averaged MSIO index and SST field. This pattern is characterized by noticeable positive values in the southwest South Atlantic, which demonstrates that the decadal variability in MSIO SST is only closely linked to midlatitude South Atlantic.

The ATL_VARMIX simulations (Atlantic Pacemaker experiment: run with AGCM coupled to a slab ocean over the Indo-Pacific region and with SST following the observed history in the Atlantic) can be employed to investigate Atlantic forcing on the Indo-Pacific region. As seen in Figure 1e, the observed decadal fluctuations in MSIO SST are well reproduced by the ATL_VARMIX simulations, and the decadal-scale positive correlation between the SAMV and MSIO SST indices is also well captured ($r = 0.83$, above the 95% confidence level). Furthermore, the spatial patterns of the SAMV-MSIO SST relationship in simulations are examined in Figures 1d and 1f, which are consistent with observations, although the simulated positive correlations in the MSIO are shifted slightly south. Given that reliable observations over the middle to high latitudes of the Southern Hemisphere are scarce, and that the ATL_VARMIX experiment performs well in reproducing

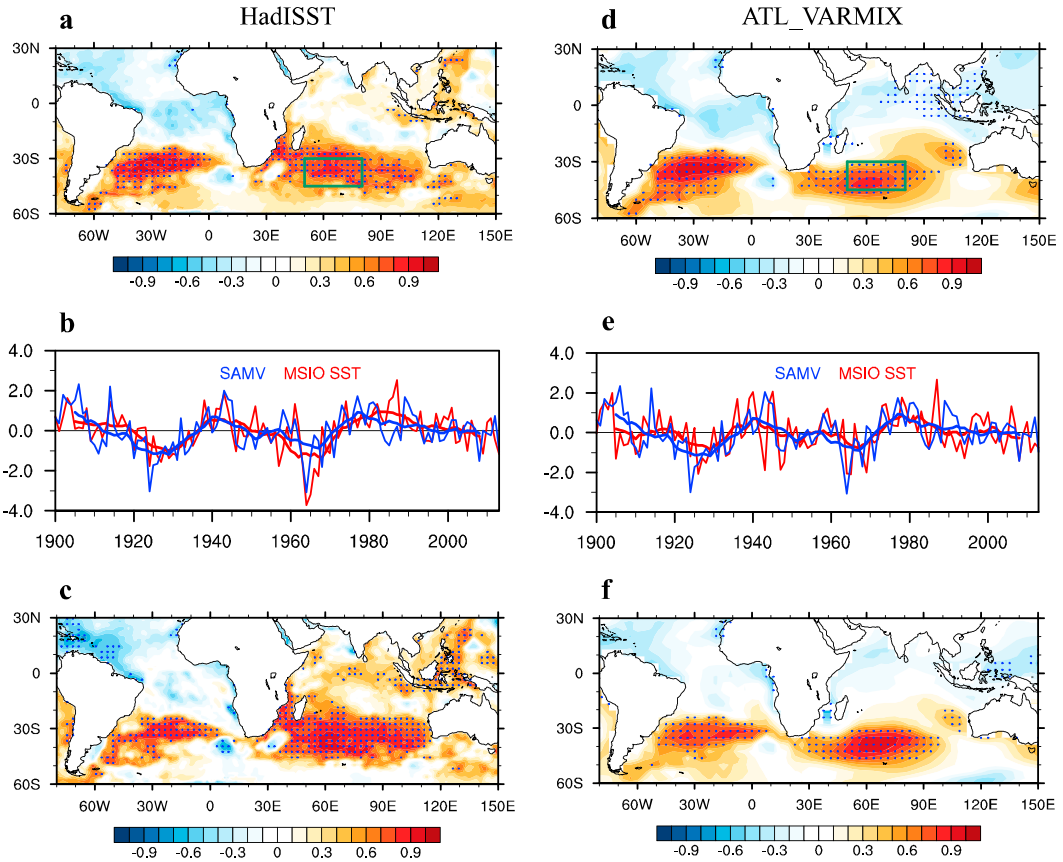

Figure 1. (a) Decadal-scale correlation map between the detrended SAMV index and SST field over the Atlantic and Indian Ocean regions, based on the HadISST data set. The boxed area represents a key domain (30°–45°S, 50°–80°E) in the MSIO, described in the main text. (b) Normalized time series of detrended SAMV and MSIO SST indices during 1900–2013 and their 11-year running means. (c) As in Figure 1a, except for the correlation between the MSIO SST index and SST field. (d–f) As in Figures 1a–1c, but derived from the ATL_VARMIX simulations. Stippling indicates correlations significant at the 95% confidence level. SAMV = South Atlantic multidecadal variability; SST = sea surface temperature; HadISST = Hadley Centre SST; MSIO = midlatitude south Indian Ocean.

the multidecadal fluctuations in MSIO SST, modeling results are employed here to explore the thermodynamic mechanism underlying the decadal variability in MSIO SST.

To explore specific physical processes driving the decadal variation in MSIO SST, surface heat budget over the MSIO is analyzed in ATL_VARMIX simulations by regressing net surface heat flux and four heat flux components onto the decadal MSIO SST index. As seen from supporting information Figure S5a, the warming in MSIO SST is driven by positive net heat flux into the ocean. Further inspection of four heat flux components indicates that MSIO SST increases are caused primarily by increased fluxes of sensible heat and longwave radiation into the ocean, while anomalous latent heat flux cools the SST (Figures 2a–2d). Figure 2e presents anomalous SLP and surface winds accompanying the MSIO warming; the MSIO is found to be located to the south of an anomalous cyclonic circulation. The easterly wind anomalies over the MSIO decrease surface wind speed (supporting information Figure S5b) and thus reduce sensible heat flux from the ocean, warming the MSIO SST. For the latent heat flux, although wind speed decreases over the MSIO, increased latent heat loss is observed. This is because positive SST anomalies in MSIO increases specific humidity difference between the sea surface and near-surface atmosphere (supporting information Figure S5d), the effect of specific humidity difference here is more dominant and thus increases latent heat loss from the ocean. Accompanying the increased surface evaporation, column-integrated water vapor is found to increase remarkably over the MSIO (Figure 2f). However, the center of water vapor anomaly shows a northward shift compared to that of evaporation; this shift is due to the transport of water vapor by

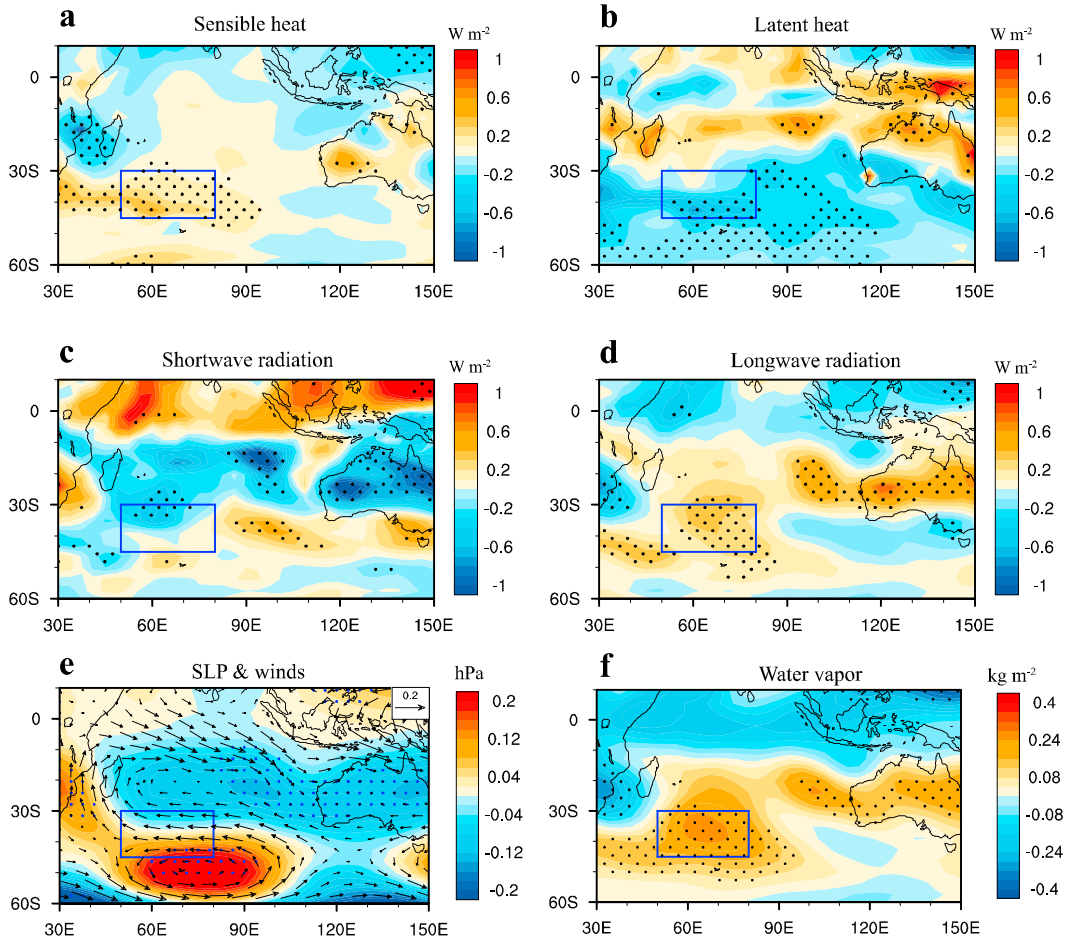

Figure 2. Regression patterns of surface (a) sensible heat flux (shading, W/m^2), (b) latent heat flux (shading, W/m^2), (c) net shortwave radiation (shading, W/m^2), (d) net longwave radiation (shading, W/m^2), (e) sea level pressure (shading, hPa) and surface winds (vectors, m/s), and (f) column-integrated water vapor (shading, kg/m^2) onto the normalized MSIO sea surface temperature index over decadal timescales in the ATL_VARMIX simulations. All fluxes are defined to be positive downward. Boxes indicate the key domain in the MSIO. Stippling denotes regressions significant at the 90% confidence level. MSIO = midlatitude south Indian Ocean; SLP = sea level pressure.

anomalous southerly winds over the MSIO (supporting information Figure S5e). Because water vapor is an important greenhouse gas, increased water vapor content in air traps more longwave radiation and results in a net longwave radiation anomaly into the ocean, thus warming MSIO SST (Figure 2d). The above results suggest the existence of a SST-water vapor-longwave radiation feedback over the MSIO; that is, warm SST anomalies increase atmospheric water vapor through enhanced surface evaporation, which then leads to increased net longwave radiation into the ocean, reinforcing the warm SST anomalies. Based on these analyses, it is hypothesized here that MSIO warming is first triggered by turbulent heat fluxes through atmospheric circulation and further amplified by a local SST-water vapor-longwave radiation thermodynamic positive feedback.

The existence of a thermodynamic positive feedback over the MSIO may amplify the MSIO SST response to SAMV forcing. Thus, the primary focus of this work is to investigate how this positive feedback is triggered by remote forcing from the South Atlantic. First, direct atmospheric responses to SAMV-related SST forcing are explored with the ATL_VARAGCM experiment (AGCM forced with observational SST over the Atlantic basin and with climatological SST over basins outside the Atlantic). In the ATL_VARAGCM simulations, the convective precipitation response to SAMV forcing displays a meridional dipolar structure over the Atlantic basin with increased (decreased) precipitation in the midlatitude (tropical) South Atlantic. Accompanying

this precipitation change, the regressed pattern of upper-level velocity potential is dominated by a positive center over tropical Africa. Thus, upper-level divergent wind anomalies are observed to flow from the midlatitude South Atlantic northward to tropical Africa (Figure 3a), indicating the occurrence of anomalous sinking over this region (supporting information Figure S6a). In addition, the regressed pattern of low-level circulation shows a clear dipolar perturbation in SLP over the South Atlantic with high (low) pressure anomalies in the north (south), indicating that an anomalous southward flow appears between these two poles (Figure 3b). Such a collocation of precipitation and circulation anomalies suggests that SAMV-related midlatitude SST anomalies may impact tropical rainfall by modulating regional meridional circulation over the South Atlantic. To investigate this possibility, supporting information Figure S7 examines SAMV related changes in meridional streamfunction and vertical motion. As expected, the SAMV forcing weakens meridional circulation over the South Atlantic and thus induces significant ascending motion over the midlatitude South Atlantic and descending motion over the tropical Atlantic. To more clearly demonstrate the role of SAMV-related midlatitude SST variability in forcing the tropical precipitation, we also conducted an experiment forced by observational SST prescribed over extratropical South Atlantic and climatological SST prescribed over basins outside the extratropical South Atlantic (supporting information Text S1). The simulation results from this experiment show that SAMV-related midlatitude SST forcing can indeed cause changes in tropical rainfall (supporting information Figure S8). Therefore, the above results demonstrate that SST warming in midlatitude South Atlantic can reduce tropical rainfall by weakening regional meridional circulation; this is consistent with the findings of Lopez, Dong, Lee, and Goni (2016).

As demonstrated in Figure 3a, the regressed pattern of precipitation indicates a prominent reduction in convection over tropical Africa, which cools the tropospheric column and drives a Matsuno-Gill pattern in tropical circulation (Kucharski et al., 2009). The equatorial Rossby wave and Kelvin wave responses then correspond to anomalous low-level easterlies over the tropical Atlantic and westerlies penetrating into the tropical Indian Ocean, respectively (Figure 3b). Due to surface friction in the boundary layer, the Kelvin wave induces anomalous southwesterly (northwesterly) surface winds on the northern (southern) side of the equator, resulting in low-level divergence over the equatorial Indian Ocean and convergence over off-equatorial regions (supporting information Figure S6b). The Kelvin-wave-induced Ekman convergence over the tropical south Indian Ocean then forces an anomalous cyclonic circulation over this region. Moreover, surface convergence over the tropical south Indian Ocean leads to an enhanced ascending motion and intensified deep convection over this region (supporting information Figure S6a and Figure 3a), which further strengthens the cyclonic response with the help of convection-circulation feedback (Xie et al., 2009). The MSIO is located on the southern side of this anomalous cyclonic circulation and is thus impacted by anomalous easterlies, which reduce the surface wind speed and corresponding turbulent heat fluxes from the ocean (supporting information Figure S9), therefore triggering the warming in MSIO SST.

The above analysis shows that the SAMV can trigger an increase in MSIO SST through an atmospheric bridge emanating from the South Atlantic. This initial warming is further amplified by a local SST-water vapor-longwave radiation thermodynamic positive feedback over the MSIO. Once the MSIO SST is warmed, it can also affect overlying atmospheric circulation. Figure 3c further examines the atmospheric response to SAMV forcing in the ATL_VARMIX experiment, which includes the local air-sea coupling over basins outside the Atlantic. Comparing Figures 3c and 3b, a high-pressure anomaly is observed over the south Indian Ocean in the ATL_VARMIX simulation, which is not present in the ATL_VARAGCM results. Because the ATL_VARMIX differs from ATL_VARAGCM only in considering the effects of local air-sea coupling over the Indo-Pacific region, the formation of this high-pressure anomaly over the south Indian Ocean can be ascribed to a feedback from MSIO warming. To confirm this inference, a sensitivity experiment utilizing the ICTPAGCM was conducted to investigate the atmospheric response to MSIO warming (supporting information Text S2) (Sutton & Hodson, 2007). As presented in supporting information Figure S10, MSIO warming does lead to a high-pressure response over the south Indian Ocean; this is consistent with the results in Reason et al. (1998). The actual atmospheric response to SAMV forcing over the Indo-Pacific region includes the impacts of feedback from the ocean. It is found, after considering local air-sea coupling, that the simulated patterns of SLP and surface winds from the ATL_VARMIX simulations are similar to the SAMV-related circulation pattern in reanalysis data sets (supporting information Figure S11). This further demonstrates the capability of the coupled model to simulate the reality.

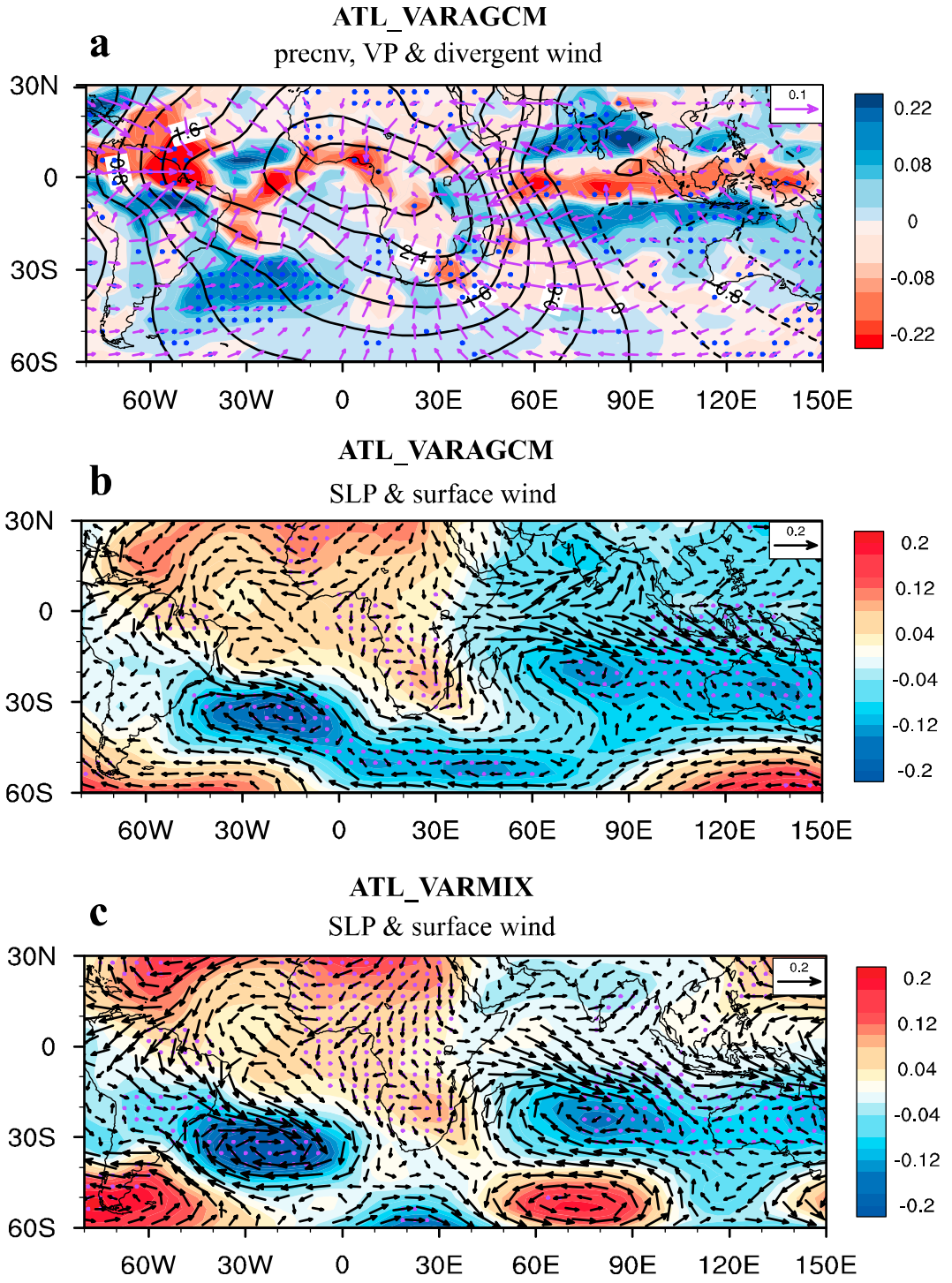

Figure 3. (a) Regressed patterns of convective precipitation (shading, mm/day), 200-hPa velocity potential (contours, 10^5 m^2/s), and divergent winds (vectors, m/s) on the normalized South Atlantic multidecadal variability index on decadal timescales in the ATL_VARAGCM simulations. (b) As in Figure 3a, but for sea level pressure (shading, hPa) and surface winds (vectors, m/s). (c) As in Figure 3b, but derived from the ATL_VARMIX simulations. Stippling indicates regressions significant at the 90% confidence level. VP = velocity potential; SLP = sea level pressure.

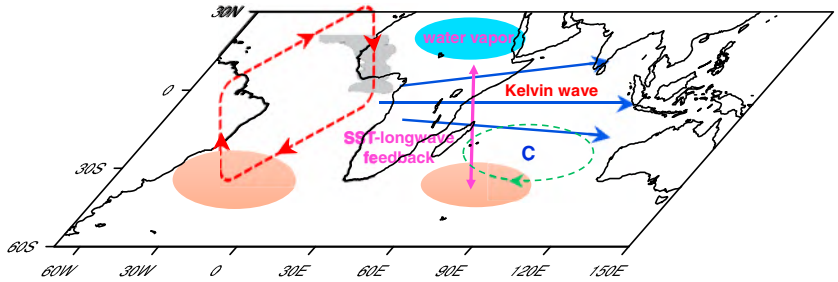

Figure 4. Schematic representation of the mechanism of transbasin connection between the South Atlantic and MSIO SST decadal variability. SST warming associated with the South Atlantic multidecadal variability (orange patch in the South Atlantic) results in weakened regional meridional circulation over the South Atlantic, suppressing convection over tropical Africa. The cold Kelvin wave then leads to the formation of a local anomalous cyclone (green circle) over the tropical south Indian Ocean, which decreases surface westerlies over the MSIO and triggers the warming in MSIO SST (orange patch in the Indian Ocean). This initial SST warming gets further amplified by a local SST-water vapor-longwave radiation positive feedback. See text for details. MSIO = midlatitude south Indian Ocean.

4. Summary and Discussion

This study provides both observational evidence and numerical experiments to demonstrate that the decadal variation in MSIO SST can be explained by remote forcing from the SAMV. The physical mechanism underlying this transbasin teleconnection is explored by employing a suite of Atlantic Pacemaker experiments and is summarized by a schematic diagram in Figure 4. As depicted in the figure, SST warming in the midlatitude South Atlantic leads to a weakening of regional meridional circulation over the South Atlantic, suppressing convection over tropical Africa. The reduced precipitation then drives a cold atmospheric Kelvin wave wedge to the east, with anomalous low-level westerlies penetrating into the tropical Indian Ocean. Under the impact of surface friction, Kelvin-wave-induced Ekman convergence occurs over the tropical south Indian Ocean and leads to the formation of a local anomalous cyclonic circulation, which weakens the westerlies over the MSIO and subsequently triggers the warming in MSIO SST. Moreover, South Atlantic forced SST warming in the MSIO is further amplified by a local SST-water vapor-longwave radiation thermodynamic positive feedback over the MSIO.

Many previous studies have noted the interannual covariability in the South Atlantic and Indian Ocean SST, which is suggested to be associated with the subtropical dipole mode (Fauchereau et al., 2003; Hermes & Reason, 2005; Morioka et al., 2012, 2014; Wang, 2010). However, the subtropical dipole mode exists only on interannual and not on decadal time scales (supporting information Figure S12). Moreover, anomalous atmospheric circulation accompanying the SAMV on interannual time scales show patterns divergent to that on decadal time scales (supporting information Figure S11, 13), which indicates that SST connection on these two time scales may be caused by different mechanisms. The interannual covariability is caused by consistent atmospheric forcing, while as suggested in this study, the South Atlantic forcing is important for the decadal-scale covariability. Moreover, it is noted that the observed spectrum of SAMV is weaker than that of the Indian Ocean, so Indian Ocean decadal variability is only partly explained by the SAMV, and the intrinsic decadal variability internal to the Indian Ocean cannot be ignored (Trenary & Han, 2013). The role of ocean dynamics is not taken into consideration in our experiments; the ocean circulation such as the Antarctic Circumpolar Current and Agulhas leakage can also play important roles in linking the South Atlantic and Indian Oceans (Biastoch et al., 2015; Morioka et al., 2017). Therefore, further research employing fully coupled models is required to quantify the relative contributions of the atmospheric bridge and oceanic tunnel to the decadal-scale SST teleconnection.

Acknowledgments
We appreciate the anonymous reviewers for their helpful comments. This work was jointly sponsored by the National Key R&D Program of China (2016YFA0601801), National Natural Science Foundation of China (NSFC) Project (41790474) and SOA International Cooperation Program on Global Change and Air-Sea Interactions (GASI-IPOVAI-03). C. Sun is supported by the State Key Laboratory of Tropical Oceanography, South China Sea Institute of Oceanology, Chinese Academy of Sciences (Project No. LTO1801). We thank Dr. Fred Kucharski at ICTP for providing the ICTPAGCM simulation data. The NCEP/NCAR and 20CRv2 reanalyses were provided by NOAA and are available at https://www.esrl.noaa.gov/psd/data/gridded/. Moreover, the HadISST data set was obtained from https://www.metoffice.gov.uk/hadobs/.

References

Allan, R. J., Lindesay, J. A., & Reason, C. J. (1995). Multidecadal variability in the climate system over the Indian Ocean region during the austral summer. *Journal of Climate*, *8*(7), 1853–1873. https://doi.org/10.1175/1520-0442(1995)008%3C1853:MVITCS%3E2.0.CO;2

Biastoch, A., Durgadoo, J. V., Morrison, A. K., Sebille, E., Weijer, W., & Griffies, S. M. (2015). Atlantic multi-decadal oscillation covaries with Agulhas leakage. *Nature Communications*, *6*(1), 10082. https://doi.org/10.1038/ncomms10082

Cheung, K. K., Jiang, N., Liu, K., & Chang, L. T. C. (2015). Interdecadal shift of intense tropical cyclone activity in the Southern Hemisphere. *International Journal of Climatology*, *35*(7), 1519–1533. https://doi.org/10.1002/joc.4073

Cole, J. E., Dunbar, R. B., Mcclanahan, T. R., & Muthiga, N. A. (2000). Tropical Pacific forcing of decadal SST variability in the western Indian ocean over the past two centuries. *Science*, *287*(5453), 617–619. https://doi.org/10.1126/science.287.5453.617

Compo, G. P., Whitaker, J. S., Sardeshmukh, P. D., Matsui, N., Allan, R. J., Yin, X., et al. (2011). The twentieth century reanalysis project. *Quarterly Journal of the Royal Meteorological Society*, *137*(654), 1–28. https://doi.org/10.1002/qj.776

Dong, L., Zhou, T., Dai, A., Song, F., Wu, B., & Chen, X. (2016). The footprint of the Inter-decadal Pacific Oscillation in Indian Ocean sea surface temperatures. *Scientific Reports*, *6*(1), 21251. https://doi.org/10.1038/srep21251

Fauchereau, N., Trzaska, S., Richard, Y., Roucou, P., & Camberlin, P. (2003). Sea-surface temperature co-variability in the southern Atlantic and Indian Oceans and its connections with the atmospheric circulation in the Southern Hemisphere. *International Journal of Climatology*, *23*(6), 663–677. https://doi.org/10.1002/joc.905

Feudale, L., & Kucharski, F. (2013). A common mode of variability of African and Indian monsoon rainfall at decadal timescale. *Climate Dynamics*, *41*(2), 243–254. https://doi.org/10.1007/s00382-013-1827-4

Han, W., Vialard, J., McPhaden, M. J., Lee, T., Masumoto, Y., Feng, M., & de Ruijter, W. P. M. (2014). Indian Ocean decadal variability: A review. *Bulletin of the American Meteorological Society*, *95*(11), 1679–1703. https://doi.org/10.1175/BAMS-D-13-00028.1

Hermes, J., & Reason, C. (2005). Ocean model diagnosis of interannual coevolving SST variability in the south Indian and South Atlantic Oceans. *Journal of Climate*, *18*(15), 2864–2882. https://doi.org/10.1175/JCLI3422.1

Kalnay, E., Kanamitsu, M., Kistler, R., Collins, W., Deaven, D., Gandin, L., et al. (1996). The NCEP/NCAR 40-year reanalysis project. *Bulletin of the American Meteorological Society*, *77*(3), 437–471. https://doi.org/10.1175/1520-0477(1996)077%3C0437:TNYRP%3E2.0.CO;2

Krishnamurthy, L., & Krishnamurthy, V. (2016). Decadal and interannual variability of the Indian Ocean SST. *Climate Dynamics*, *46*(1–2), 57–70. https://doi.org/10.1007/s00382-015-2568-3

Kucharski, F., Bracco, A., Yoo, J. H., Tompkins, A., Feudale, L., Ruti, P., & Dell'Aquila, A. (2009). A Gill-Matsun-type mechanism explains the tropical Atlantic influence on African and Indian monsoon rainfall. *Quarterly Journal of the Royal Meteorological Society*, *135*(640), 569–579. https://doi.org/10.1002/qj.406

Kucharski, F., Ikram, F., Molteni, F., Farneti, R., Kang, I. S., No, H. H., et al. (2016). Atlantic forcing of Pacific decadal variability. *Climate Dynamics*, *46*(7–8), 2337–2351. https://doi.org/10.1007/s00382-015-2705-z

Kucharski, F., Parvin, A., Rodriguezfonseca, B., Farneti, R., Martinrey, M., Polo, I., et al. (2016). The teleconnection of the tropical Atlantic to Indo-Pacific sea surface temperatures on inter-annual to centennial time scales: A review of recent findings. *Atmosphere*, *7*(2), 29. https://doi.org/10.3390/atmos7020029

Le Bars, D., Viebahn, J., & Dijkstra, H. (2016). A Southern Ocean mode of multidecadal variability. *Geophysical Research Letters*, *43*, 2102–2110. https://doi.org/10.1002/2016GL068177

Lee, S.-K., Park, W., Baringer, M. O., Gordon, A. L., Huber, B., & Liu, Y. (2015). Pacific origin of the abrupt increase in Indian Ocean heat content during the warming hiatus. *Nature Geoscience*, *8*(6), 445–449. https://doi.org/10.1038/ngeo2438

Li, J., Sun, C., & Jin, F. F. (2013). NAO implicated as a predictor of Northern Hemisphere mean temperature multidecadal variability. *Geophysical Research Letters*, *40*, 5497–5502. https://doi.org/10.1002/2013GL057877

Lopez, H., Dong, S., Lee, S. K., & Campos, E. (2016). Remote influence of Interdecadal Pacific Oscillation on the South Atlantic meridional overturning circulation variability. *Geophysical Research Letters*, *43*(15), 8250–8258. https://doi.org/10.1002/2016GL069067

Lopez, H., Dong, S., Lee, S.-K., & Goni, G. (2016). Decadal modulations of interhemispheric global atmospheric circulations and monsoons by the South Atlantic meridional overturning circulation. *Journal of Climate*, *29*(5), 1831–1851. https://doi.org/10.1175/JCLI-D-15-0491.1

Marshall, J., & Speer, K. (2012). Closure of the meridional overturning circulation through Southern Ocean upwelling. *Nature Geoscience*, *5*(3), 171–180. https://doi.org/10.1038/ngeo1391

Morioka, Y., Engelbrecht, F., & Behera, S. K. (2015). Potential sources of decadal climate variability over southern Africa. *Journal of Climate*, *28*(22), 8695–8709. https://doi.org/10.1175/JCLI-D-15-0201.1

Morioka, Y., Masson, S., Terray, P., Prodhomme, C., Behera, S. K., & Masumoto, Y. (2014). Role of tropical SST variability on the formation of subtropical dipoles. *Journal of Climate*, *27*(12), 4486–4507. https://doi.org/10.1175/JCLI-D-13-00506.1

Morioka, Y., Taguchi, B., & Behera, S. K. (2017). Eastward propagating decadal temperature variability in the South Atlantic and Indian Oceans. *Journal of Geophysical Research: Oceans*, *122*, 5611–5623. https://doi.org/10.1002/2017JC012706

Morioka, Y., Tozuka, T., Masson, S., Terray, P., Luo, J.-J., & Yamagata, T. (2012). Subtropical dipole modes simulated in a coupled general circulation model. *Journal of Climate*, *25*(12), 4029–4047. https://doi.org/10.1175/JCLI-D-11-00396.1

Nnamchi, H. C., Li, J., Kucharski, F., Kang, I.-S., Keenlyside, N. S., Chang, P., & Farneti, R. (2016). An equatorial–extratropical dipole structure of the Atlantic Niño. *Journal of Climate*, *29*(20), 7295–7311. https://doi.org/10.1175/JCLI-D-15-0894.1

Rayner, N., Parker, D. E., Horton, E., Folland, C., Alexander, L., Rowell, D., et al. (2003). Global analyses of sea surface temperature, sea ice, and night marine air temperature since the late nineteenth century. *Journal of Geophysical Research*, *108*(D14), 4407. https://doi.org/10.1029/2002JD002670

Reason, C. (2000). Multidecadal climate variability in the subtropics/mid-latitudes of the Southern Hemisphere oceans. *Tellus A*, *52*(2), 203–223. https://doi.org/10.3402/tellusa.v52i2.12259

Reason, C., Godfred-Spenning, C., Allan, R., & Lindesay, J. (1998). Air-sea interaction mechanisms and low-frequency climate variability in the south Indian Ocean region. *International Journal of Climatology*, *18*(4), 391–405. https://doi.org/10.1002/(SICI)1097-0088(19980330)18:4%3C391::AID-JOC253%3E3.0.CO;2-C

Sun, C., Kucharski, F., Li, J., Jin, F.-F., Kang, I.-S., & Ding, R. (2017). Western tropical Pacific multidecadal variability forced by the Atlantic multidecadal oscillation. *Nature Communications*, *8*, 15998. https://doi.org/10.1038/ncomms15998

Sun, C., Li, J., Ding, R., & Jin, Z. (2016). Cold season Africa–Asia multidecadal teleconnection pattern and its relation to the Atlantic multidecadal variability. *Climate Dynamics*, *48*(11–12), 3903–3918. https://doi.org/10.1007/s00382-016-3309-y

Sutton, R. T., & Hodson, D. L. (2007). Climate response to basin-scale warming and cooling of the North Atlantic Ocean. *Journal of Climate*, *20*(5), 891–907. https://doi.org/10.1175/JCLI4038.1

Tozuka, T., Luo, J., Masson, S., & Yamagata, T. (2007). Decadal modulations of the Indian Ocean dipole in the SINTEX-F1 coupled GCM. *Journal of Climate*, *20*(13), 2881–2894. https://doi.org/10.1175/JCLI4168.1

Trenary, L., & Han, W. (2013). Local and remote forcing of decadal sea level and thermocline depth variability in the south Indian Ocean. *Journal of Geophysical Research: Oceans*, *118*, 381–398. https://doi.org/10.1029/2012JC008317

Trenberth, K. E., & Fasullo, J. T. (2013). An apparent hiatus in global warming? *Earth's Future*, *1*(1), 19–32. https://doi.org/10.1002/2013EF000165

Venegas, S. A., Mysak, L. A., & Straub, D. N. (1998). An interdecadal climate cycle in the South Atlantic and its links to other ocean basins. *Journal of Geophysical Research*, *103*(C11), 24,723–24,736. https://doi.org/10.1029/98JC02443

Wainer, I., & Venegas, S. A. (2002). South Atlantic multidecadal variability in the climate system model. *Journal of Climate*, *15*(12), 1408–1420. https://doi.org/10.1175/1520-0442(2002)015%3C1408:SAMVIT%3E2.0.CO;2

Wang, F. (2010). Subtropical dipole mode in the Southern Hemisphere: A global view. *Geophysical Research Letters*, *37*, L10702. https://doi.org/10.1029/2010GL042750

Xie, S.-P., Hu, K., Hafner, J., Tokinaga, H., Du, Y., Huang, G., & Sampe, T. (2009). Indian Ocean capacitor effect on Indo–western Pacific climate during the summer following El Niño. *Journal of Climate*, *22*(3), 730–747. https://doi.org/10.1175/2008JCLI2544.1

Xue, F. (2001). Interannual to interdecadal variation of East Asian summer monsoon and its association with the global atmospheric circulation and sea surface temperature. *Advances in Atmospheric Sciences*, *18*(4), 567–575. https://doi.org/10.1007/s00376-001-0045-x

Xue, J., Li, J., Sun, C., Zhao, S., Mao, J., Dong, D., et al. (2018). Decadal-scale teleconnection between South Atlantic SST and southeast Australia surface air temperature in austral summer. *Climate Dynamics*, *50*, 2687–2703. https://doi.org/10.1007/s00382-017-3764-0

Zhang, H., Wen, Z., Wu, R., Chen, Z., & Guo, Y. (2017). Inter-decadal changes in the East Asian summer monsoon and associations with sea surface temperature anomaly in the south Indian Ocean. *Climate Dynamics*, *48*(3–4), 1125–1139. https://doi.org/10.1007/s00382-016-3131-6